A Simple Neural Network Based Model Approach for Nylon 66 Fabrics Used in Safety Restraint Systems: A Comparison of Two Training Algorithms

RAMESH KESHAVARAJ,[1,*] RICHARD W. TOCK,[1] and GUY S. NUSHOLTZ[2]

[1]Polymer Processing and Testing Laboratory, Department of Chemical Engineering, Texas Tech University, Lubbock, Texas 79409-43121; [2]Chrysler Technology Center, Chrysler Corporation, Auburn Hills, Michigan 48326-2757

SYNOPSIS

Airbag technology relies on woven fabrics as the material of construction and particularly on knowledge pertaining to the fabric's permeability as a function of pressure drop, inflation temperature of the gas, fabric weave, fiber denier, and biaxial stress–strain relationships under biaxial conditions. While fabric permeability can be quantified by actual experimental measurements, the number and nonlinearity of the variables involved make the experiments time- and cost-intensive. Moreover, interpolations within a given data set can yield questionable results. In this study, a very simple feed forward neural network architecture was used with a training rule involving a nonlinear optimization routine for updating weights of the proposed network. This training was compared to the training with an error-back propagation routine. During this training, the ANN is introduced to data that contain the actual cause and effect patterns, with adjustments being made by changes in weighting factors until the errors in the output variables are minimized. Once trained, ANN can ascertain the essentials of the relationships and assimilate henceforth. In this study, after the initial training, the ANN was tested on additional data which were not part of the training processes. The predictions of the proposed trained network agreed very well with the new experimental data. On this basis, the proposed ANN model appears to be an effective tool for modeling airbag fabric behavior. This ANN model can assimilate relationships between different variables from the real-world data and does not require extensive normalizing of the process data like a back-propagation algorithm. Once trained, only fractions of a second are needed for information assimilation and output generation. This coupled with simplicity of use and accuracy of predictions from the real-world data make this ANN model attractive for on-line applications. © 1995 John Wiley & Sons, Inc.

INTRODUCTION

Airbag fabrics undergo biaxial stretching during deployment. But the performance of these fabrics under these conditions has not been widely reported in the literature. An expansible fabric, stretched biaxially, will open up and become more permeable. The extent to which this openness changes with temperature, pressure drop, fabric weave, and fabric denier is difficult to determine a priori. Moreover, in the third generation of airbags known as "smart-bags," the energy dissipation relies primarily on permeability through the fabric rather than on vents. In this regard, the material properties of the fabric can significantly contribute to the safety of the vehicle occupant as he or she interacts with the deployed airbag. The two properties that contribute to the energy-absorbing capabilities of the fabric bag are its permeability and its biaxial stress–strain characteristics in the plane of the fabric.[1-3]

The most obvious feature of fabrics is that they have almost no bending strength and, hence, exhibit an inability to support compressive loads in the plane of the fabric. This inability to support compressive loads introduces a strong nonlinearity into any attempt to approximate a fabric as an isotropic

* To whom correspondence should be addressed.

Journal of Applied Polymer Science, Vol. 57, 1127–1144 (1995)
 CCC 0021-8995/95/091127-16

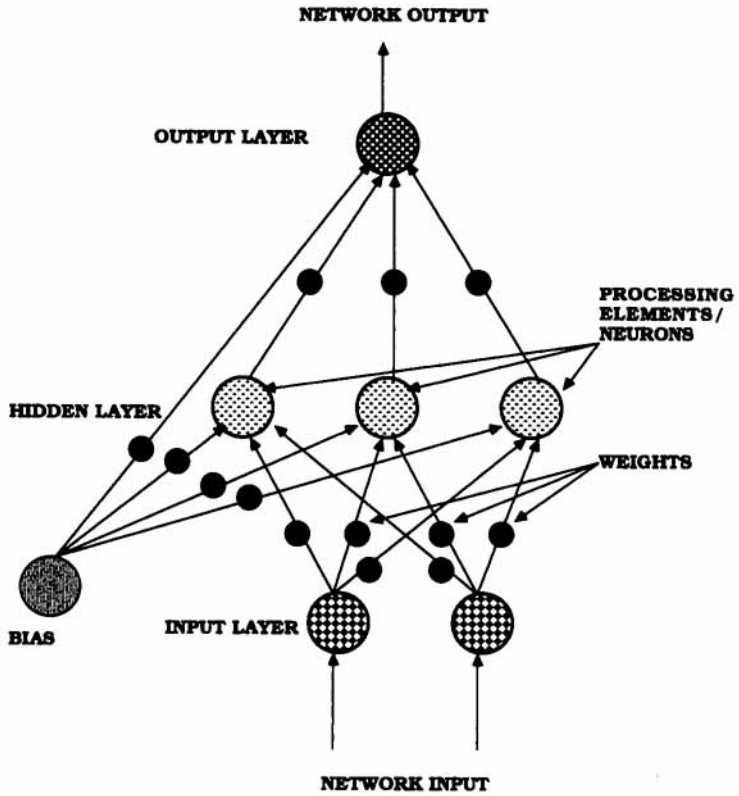

Figure 1 Schematic of a feed forward neural network architecture.

or orthotropic continua. The initial unidirectional fiber resistance is attributed to the resistance encountered during the straightening of the threads.

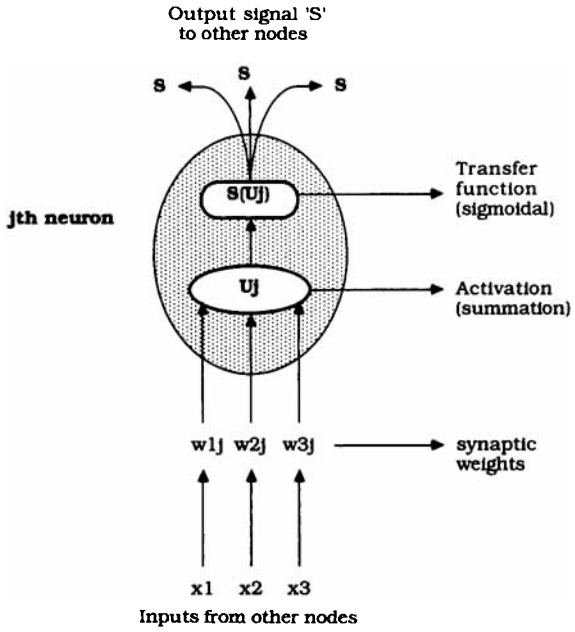

Figure 2 Anatomy of a typical neuron.

This resistance arises from the flexural rigidity of the threads under tension, while the threads in the transverse direction are forced to become more undulated by the process. An additional complicating factor is that the fibers which make up a fabric also interact in a complex manner which deviates considerably from continuum behavior. Under uniaxial tension, most of the nonlinear response is due to the kinematic interaction between the warp and weft threads and their undulation in the unstressed state. However, these effects are greatly reduced under biaxial tensile conditions.[4]

The purpose of this article was to demonstrate how a simple neural network approach was used to model complex physical behavior of airbag fabrics. The major variables are fiber denier, fabric weave,

Table I Physical Characteristics of Test Fabrics

Fabric Denier	Weave Count	Weave Type/Process
315	60 × 60	Plain
420	49 × 49	Fancy
630	41 × 41	Plain
840	32 × 32	Ripstop

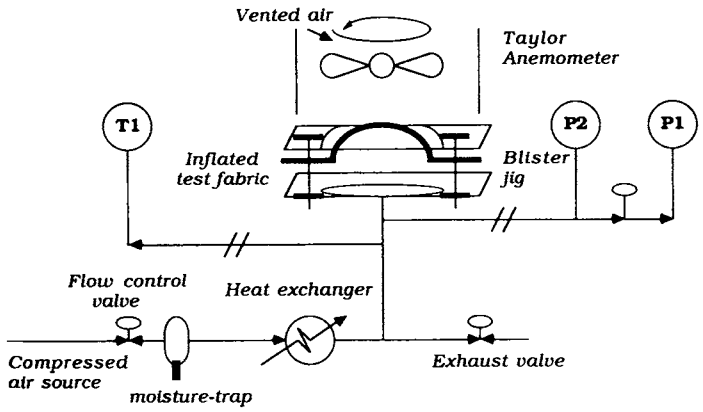

Figure 3 Schematic of the blister-inflation apparatus.

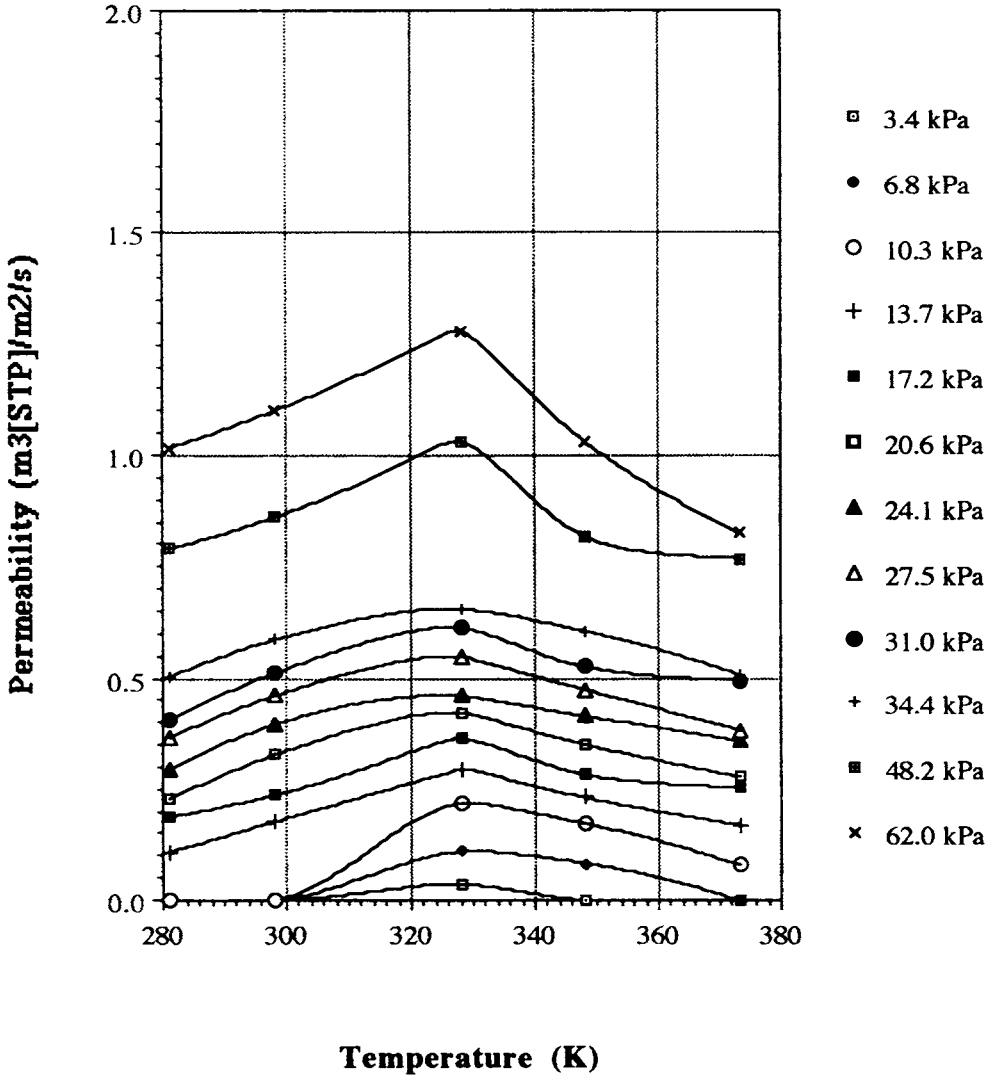

Figure 4 Permeability isobars for the 315-denier nylon 66 fabric in the low-pressure-drop experiments.

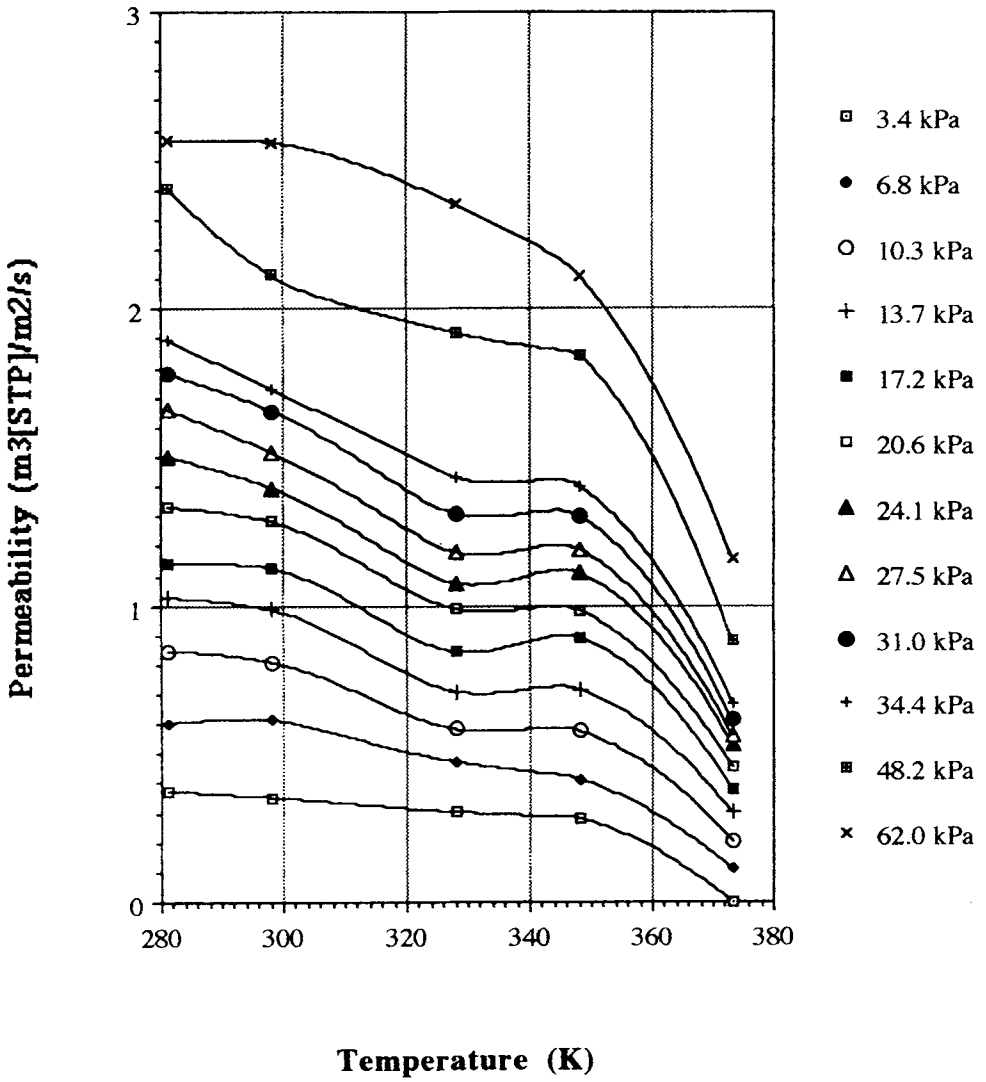

Figure 5 Permeability isobars for the 420-denier nylon 66 fabric in the low-pressure-drop experiments.

weave count, inflation temperature, and permeability for a given pressure drop.

THEORY

Blister-inflation Technique

As mentioned earlier, inelastic/elastic fiber stretching and viscous air flow through the fabric or vents in the fabric are the two mechanisms[2-5] by which energy is adsorbed by a deployed smart-airbag. Both of these mechanisms, fiber stretching and airflow through the fabric, were quantified using a blister-inflation technique in our earlier investigations.[1]

With respect to fiber stretching, the approach Tock and Nusholtz[1,2] used for the calculation of the biaxial stress and strain in distended fabrics is based on the relationships derived by Denson and coworkers for solid plastic films.[6-9] In both instances, biaxial tensile stress is calculated by the following equation:

$$\sigma_b = \frac{PD}{d_0}\left[4(x)^3 + 2(x) + \left(\frac{1}{4}\right)\left(\frac{1}{x}\right)\right] \quad (1)$$

The amount of biaxial strain is given by the following equation:

$$\varepsilon_b = \ln\left[\left\{\cos^{-1}\left(\frac{1 - 4(x)^2}{1 + 4(x)^2}\right)\right\}\left\{x + \left(\frac{1}{4}\right)\left(\frac{1}{x}\right)\right\}\right] \quad (2)$$

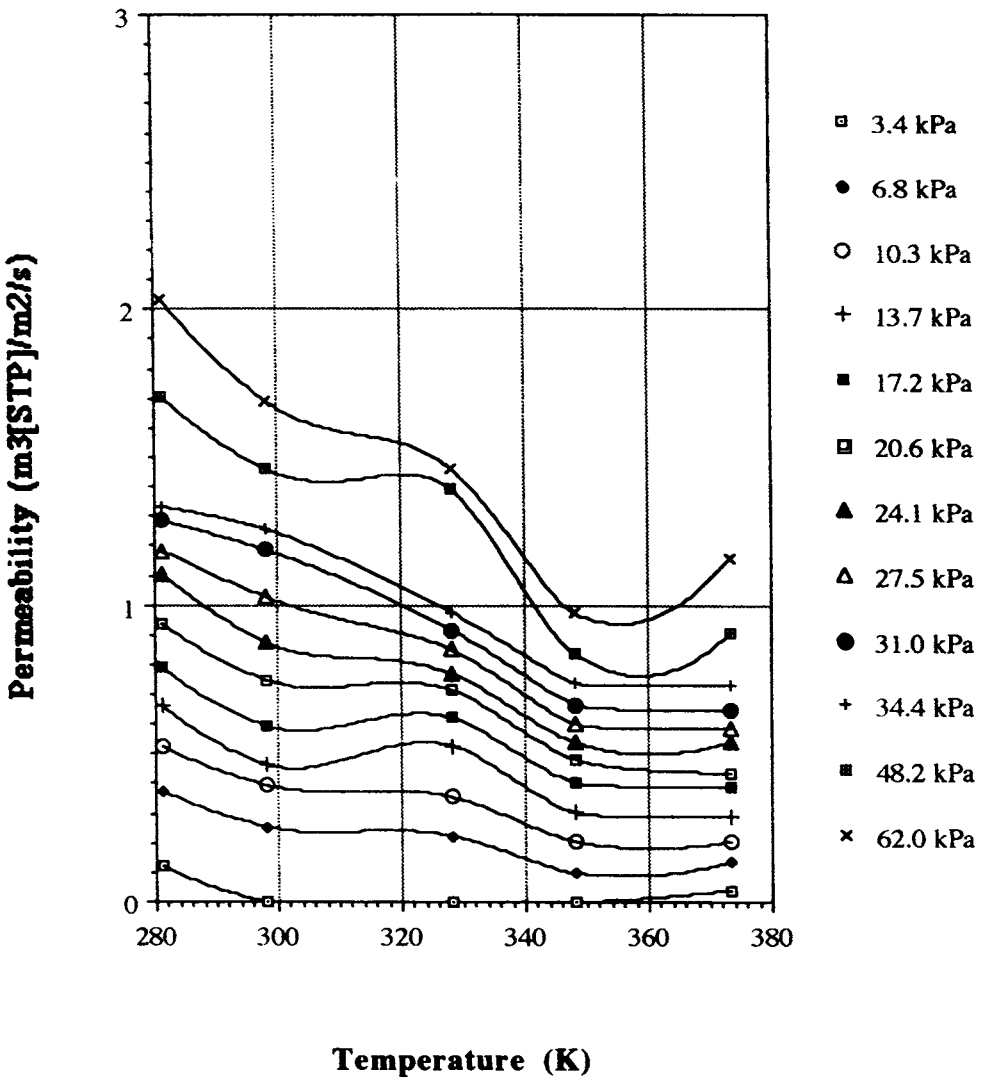

Figure 6 Permeability isobars for the 630-denier nylon 66 fabric in the low-pressure-drop experiments.

In these equations, the variables in SI units are σ_b = biaxial tensile stress in the fabric, Pa; P = pressure drop across the fabric, Pa; d_0 = the original fabric thickness, m; x = dimensional less ratio of (h/D); h = height of the blister, m; D = blister diameter, m; and ε_b = biaxial strain in the fabric. Equations (1) and (2) were derived based on the assumption that a constant volume of the polymer sheet deforms from a flat configuration into a spherical segment during the blister-inflation experiments. This same assumption applies to the woven fabric samples used in this study.

Neural Networks

Neural networks are constructed of processing elements known as neurons that are connected via information channels called interconnections. Neural nets can identify and learn correlative patterns between sets of input data and corresponding target values. Once trained, neural nets can be used to forecast the outputs expected for new levels of input variables. Each neuron can have multiple inputs, but only one output. Each output, however, branches out to input to many other neurons. The neurons operate collectively and simultaneously on most or all data and are configured in regular architecture. They "learn" by extracting preexisting information from the data that describe the relationship between the inputs and the outputs. Hence, in the learning process, the network actually acquires knowledge or information from the environment. As a result of the interrelationships, the network assimilates information that can be recalled later. Neural net-

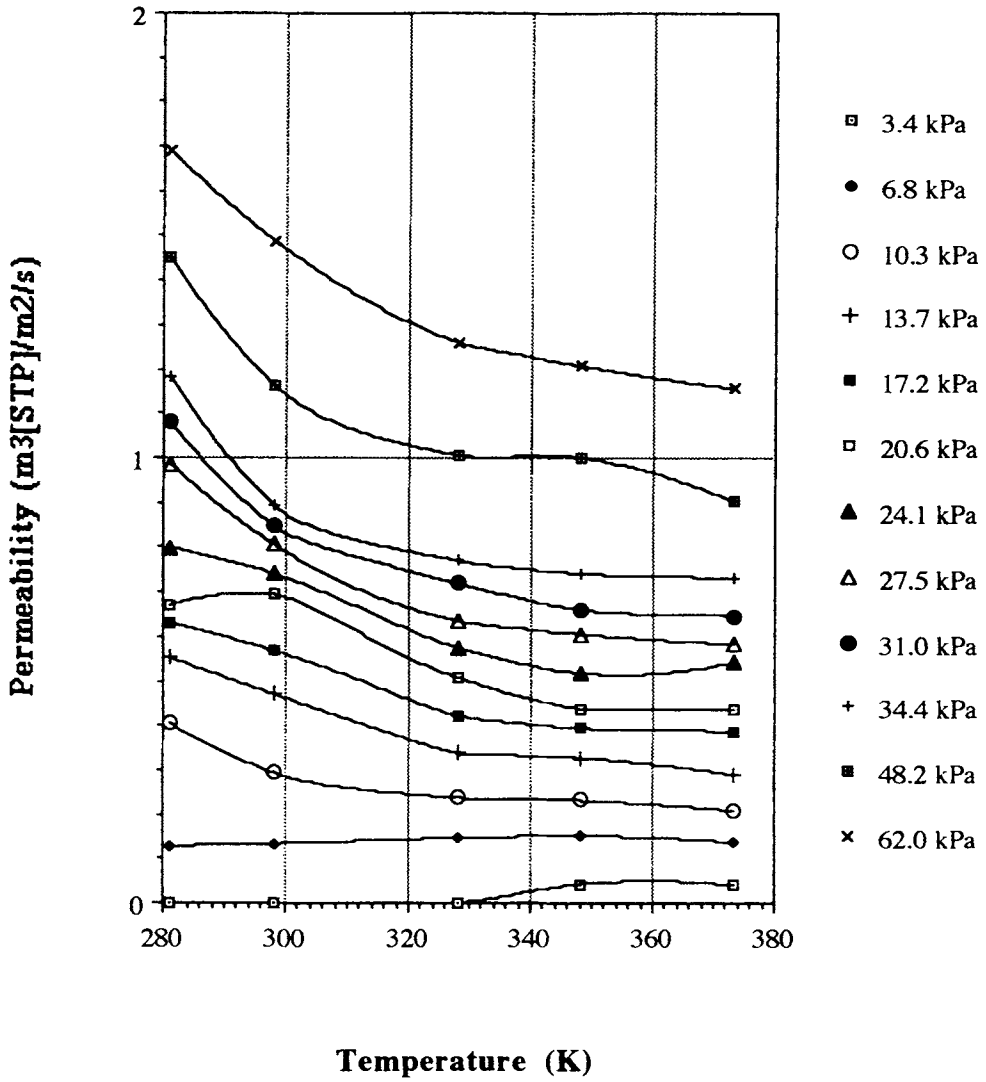

Figure 7 Permeability isobars for the 840-denier nylon 66 fabric in the low-pressure-drop experiments.

works which are capable of handling complex and nonlinear problems can process information rapidly and can reduce the engineering effort required in developing highly computation-intensive modeling, such as nonlinear FEA. Neural networks also come in a variety of types, and each have their distinct architectural differences and uses.[10]

The structure of neural nets forms the basis for information storage and governs the learning process. The type of neural network used in this work is known as a feed forward network in which a nonlinear optimization method was used to estimate the strength of each connection, i.e., weights. The training achieved through this technique was then compared to a back-propagation training which has forward flowing information in the prediction mode and back-propagated error correction in the training mode. Hence, the information flows only in the forward direction, i.e., from input to output in the testing mode. A general structure of a feed forward network is shown in Figure 1. Such connections are made between neurons of adjacent layers: A neuron is connected so that it receives signals from each neuron in the immediate preceding layer and transmits signals to each neuron in the immediate succeeding layer. Neural networks which are organized in layers typically consist of at least three layers: an input layer, one or more hidden layers, and an output layer. The input and output layers serve as interfaces which perform an appropriate scaling relationship between the actual and the network data. Hidden layers are so termed because their neurons are hid-

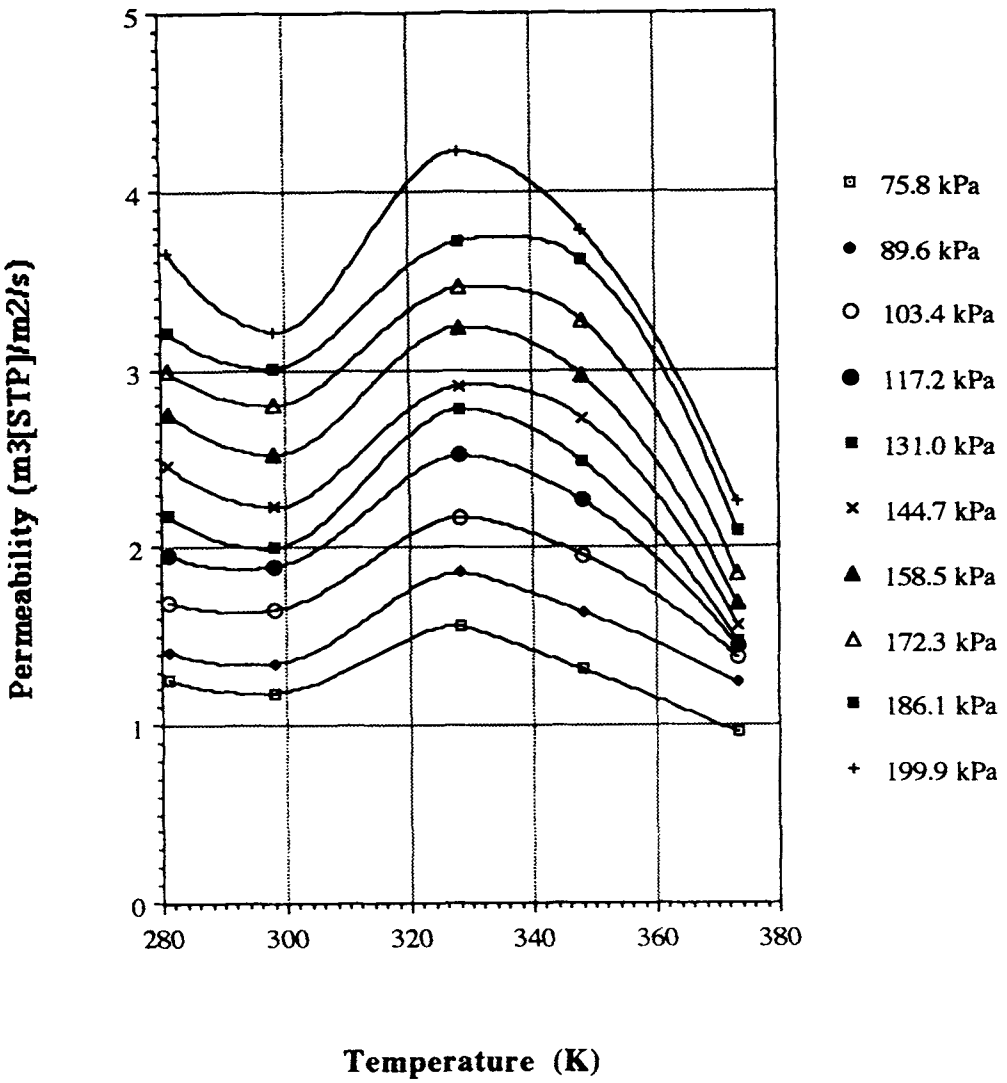

Figure 8 Permeability isobars for the 315-denier nylon 66 fabric in the high-pressure-drop experiments.

den from the actual data. The connections are the means for information flow. Each connection has an associated weight factor, w_i, expressed by a numerical value which can be adjusted. The weight is an indication of the connection strength between two neurons.

The neurons in the hidden and output layers perform summing and nonlinear mapping functions. The functions carried by each neuron are illustrated in Figure 2. Each neuron occupies a particular position in a feed forward network and accepts inputs only from other neurons and sends its outputs to other neurons. The inputs from other nodes are first summed up. This summing of the weighted inputs is carried out by a processor within the neuron. The sum that is obtained is called the activation of the neuron. Each activated neuron performs three primary functions: receives signals from other neurons, sums their signals, and transforms the sum. For example, if the output from the ith neuron with pattern p is designated as $x_{i,p}$, then the input to the jth neuron from the ith neuron is $x_{i,p}w_{i,j}$. Summing the weighted inputs to the jth neuron can be represented as

$$u_{i,p} = \sum_i x_{i,p}w_{i,j} - w_{B,j}\theta_j \tag{3}$$

where θ_j is a bias term and $w_{B,j}$ is the weight of the connection from the bias neuron to the jth neuron. This activation can be positive, zero, or negative, because the synaptic weightings and the inputs can

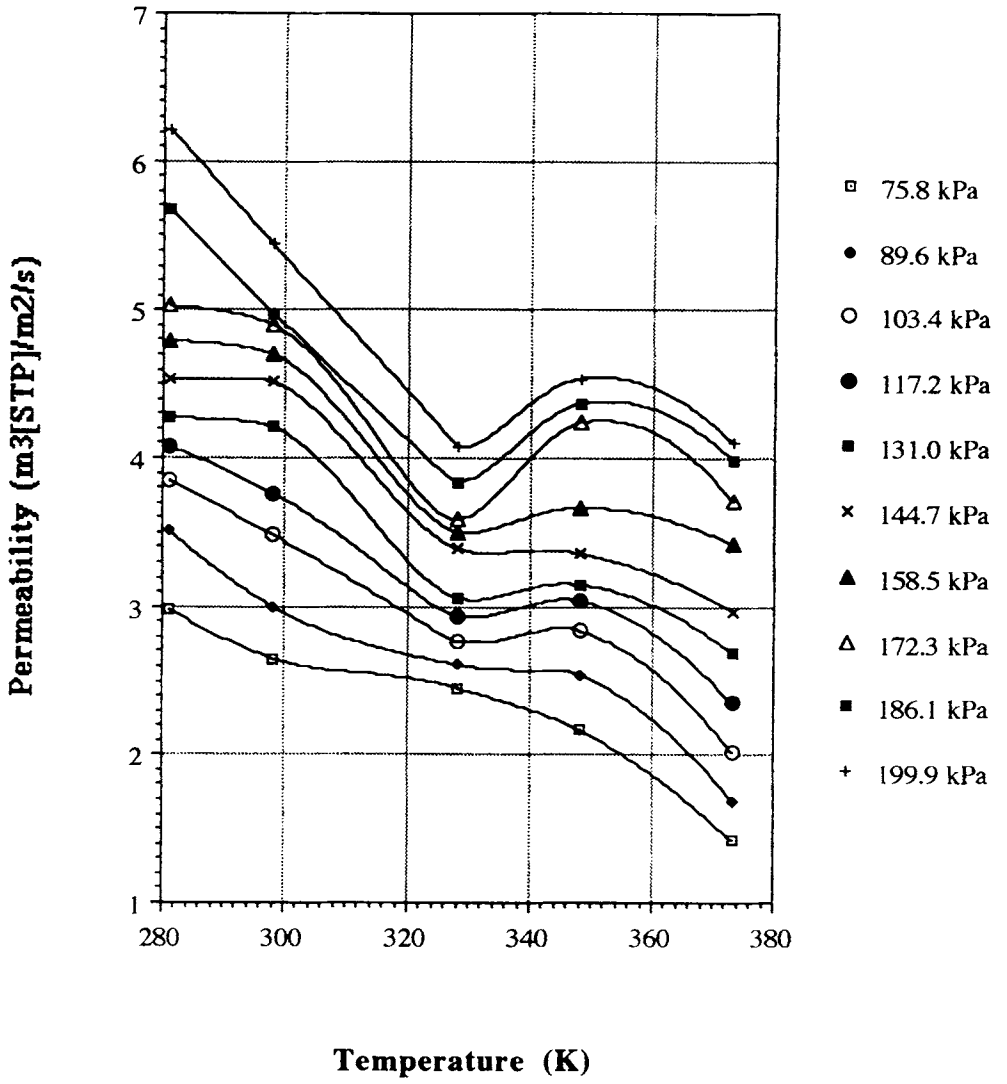

Figure 9 Permeability isobars for the 420-denier nylon 66 fabric in the high-pressure-drop experiments.

be either positive or negative. Any weighted input that makes a positive contribution to activation represents a triggering or tendency to turn the neuron on. An input making a negative contribution represents an inhibition which tends to turn the neuron off. After summing its inputs to determine its activation, the summed total is then modified by a mapping function, also known as a transfer function/threshold function. A transfer function commonly used is the "sigmoid," which is expressed as

$$S_{i,p} = \frac{1}{[1 + \exp(-u_{i,p})]} \tag{4}$$

A sigmoid (s-shaped) is a continuous function that has a derivative at all the points and is a monotonically increasing function, where $S_{i,p}$ is the transformed output asymptotic to $0 \leq S_{i,p} \leq 1$ and $u_{i,p}$ is the summed total of the inputs $(-\infty \leq u_{i,p} \leq +\infty)$ for pattern p. Hence, when the neural network is presented with a set of input data, each neuron sums up all the inputs modified by the corresponding connection weights and applies the transfer function to the summed total. This process is repeated until the network outputs are obtained.

"Training" a Neural Network

Once the network architecture is selected and the characteristics of the neurons and the initial weights are specified, the network has to be taught to associate new patterns and new functional de-

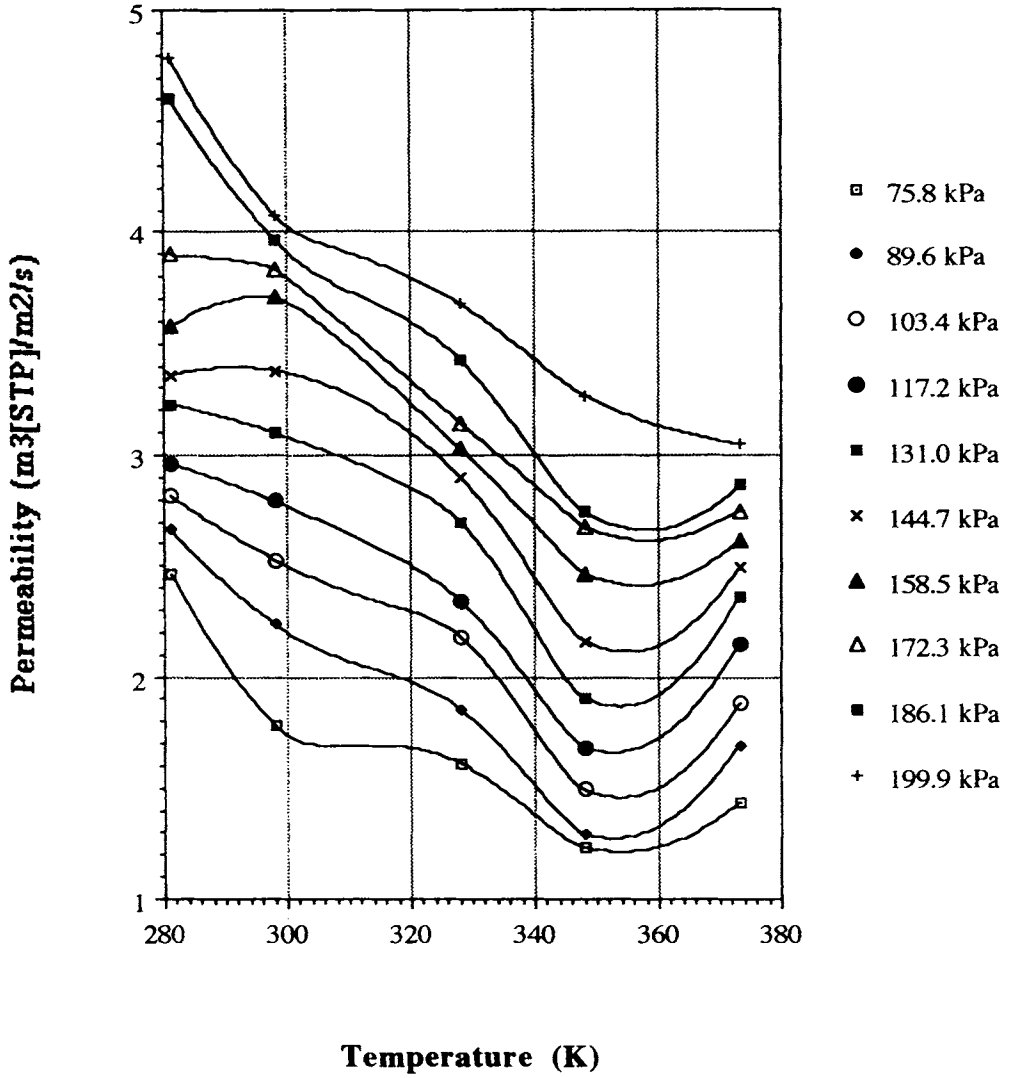

Figure 10 Permeability isobars for the 630-denier nylon 66 fabric in the high-pressure-drop experiments.

pendencies. Learning corresponds to the adjustment of the weights in order to obtain satisfactory input–output mapping. Since neural networks do not use a priori information about the process to be modeled and learning is experimental, it is necessary to have data which adequately represent the relationship between the process input and output.

Several different learning rules have been proposed by various researchers,[10] but the aim of every learning process is to adjust the weights in order to minimize the error between the network predicted output and the actual output. The output from each neuron i is $S_{i,p}$, as shown in eq. (4).

Proposed ANN Training Routine

A faster training process is to search for the weights with the help of a optimization routine that minimizes the same objective function. The learning rule used in this work is common to a standard nonlinear optimization or least-squares technique. Moreover, the entire set of weights are adjusted at once instead of adjusting them sequentially from the output to the input layers. The weight adjustment was done at the end of each exposure of the entire training set to the network, and the sum of squares of all errors for all patterns was used as the objective function for the optimization problem. A nonlinear optimization routine based on the Levenberg–Marquardt method[11] was used for solving the nonlinear

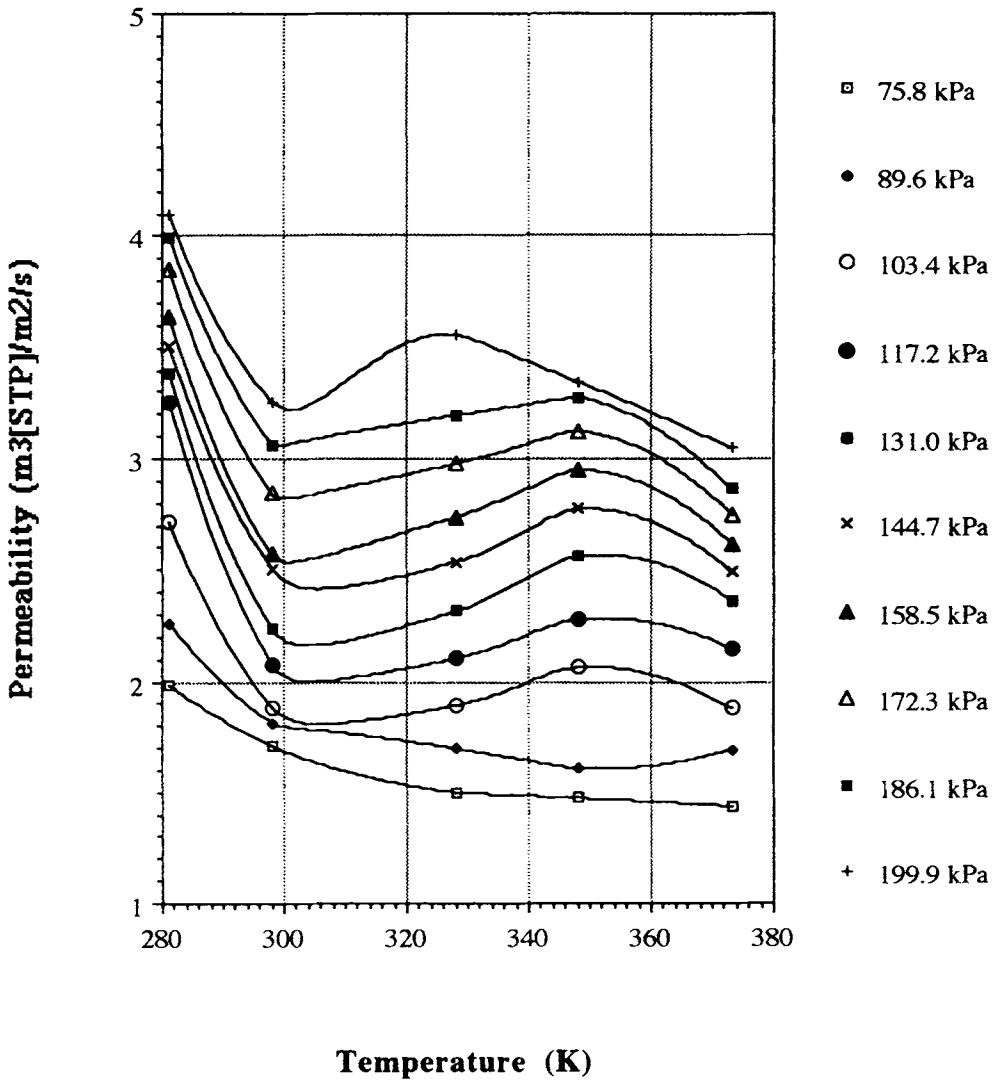

Figure 11 Permeability isobars for the 840-denier nylon 66 fabric in the high-pressure-drop experiments.

least-squares problem. The optimization problem can be defined if the model to be fitted to the data is written as follows:

$$F(y) = f(\alpha_1, \alpha_2, \ldots, \alpha_m; \beta_1, \beta_2, \ldots, \beta_k) = f(\alpha, \beta) \quad (5)$$

where $\alpha_1, \alpha_2, \ldots, \alpha_m$ are independent variables, $\beta_1, \beta_2, \ldots, \beta_k$ are the population values of the k parameter, and $F(y)$ is the expected value of the independent variable y. Then, the data points can be denoted by

$$(Y_i, X_{1i}, X_{2i}, \ldots, X_{mi})\ i = 1, 2, \ldots, n \quad (6)$$

The problem is to compute those estimates of the parameter which will minimize the following objective function:

$$\phi = \sum_{i=1}^{n} [Y_i - \hat{Y}_i]^2 \quad (7)$$

where $\hat{Y}_i$ is the value of y predicted by the model at the ith data point. The parameters to be determined in our case are the strength of the connections, i.e., the weights, w_i. More details of this Levenberg–Marquardt method can be found elsewhere.[12] This algorithm shares with the gradient methods their ability to converge from an initial guess which may be outside the range of convergence of other methods. It shares with the Taylor

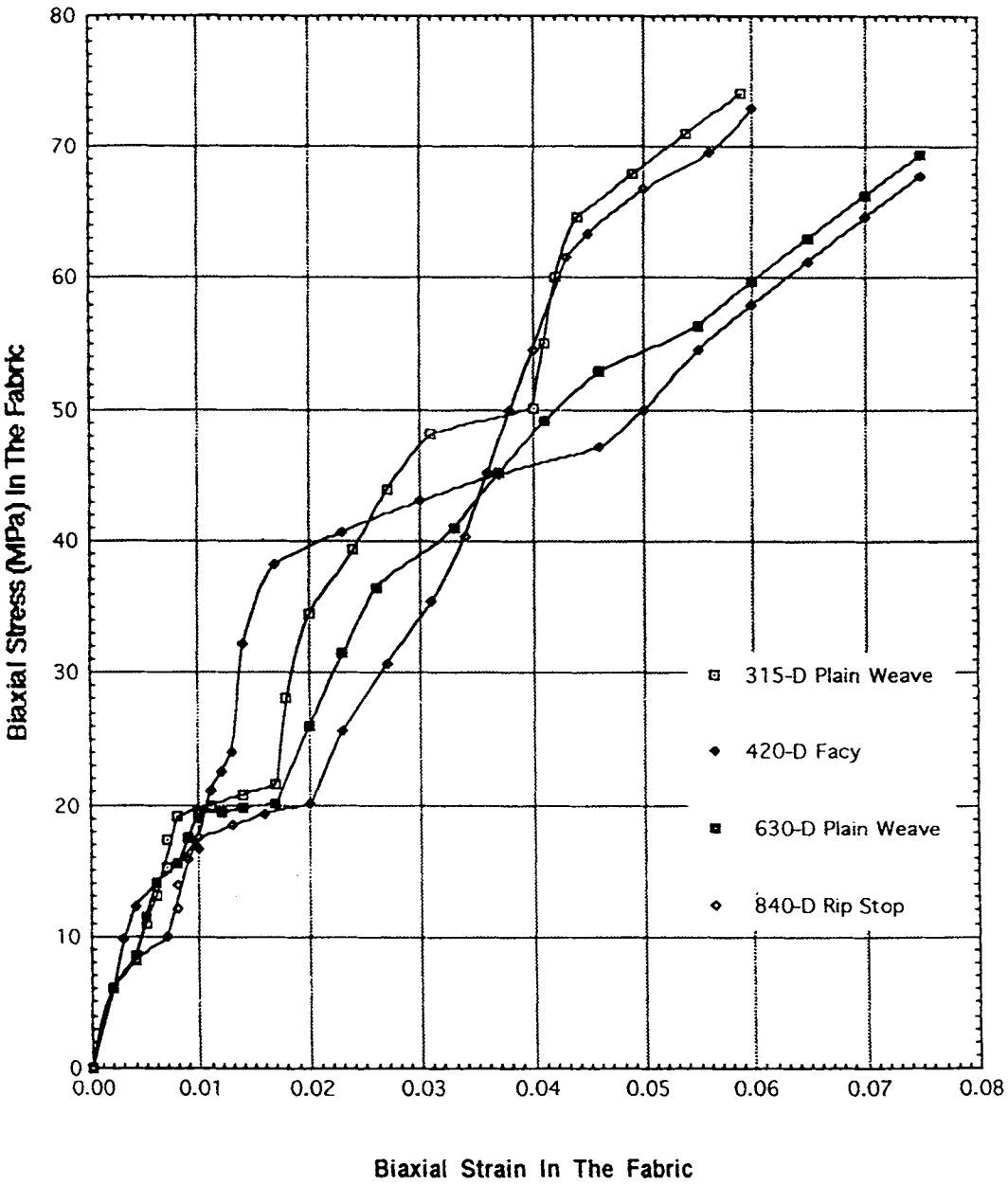

Figure 12 Biaxial stress–strain behavior of nylon 66 fabrics in blister-inflation experiments.

series method the ability to close in on the converged values rapidly after the vicinity of the converged values have been reached. The optimization procedure updated weights at every connection and yielded rapid and robust training. The weights were initialized to values in the range ±0.1 by random assignment.

Standard Error-back-propagation Routine

In a standard back-propagation scheme, updating of the weights is done iteratively. The weights for each connection are initially randomized when the neural network undergoes training. Then, the error between the target output and the network predicted output are back-propagated through the network. The back-propagation of error is used to update the connection weights. Repeated iterations of this operation results in a convergence to a set of connection weights.

The general principle behind most commonly used back-propagation learning methods is the "delta rule," by which an objective function involv-

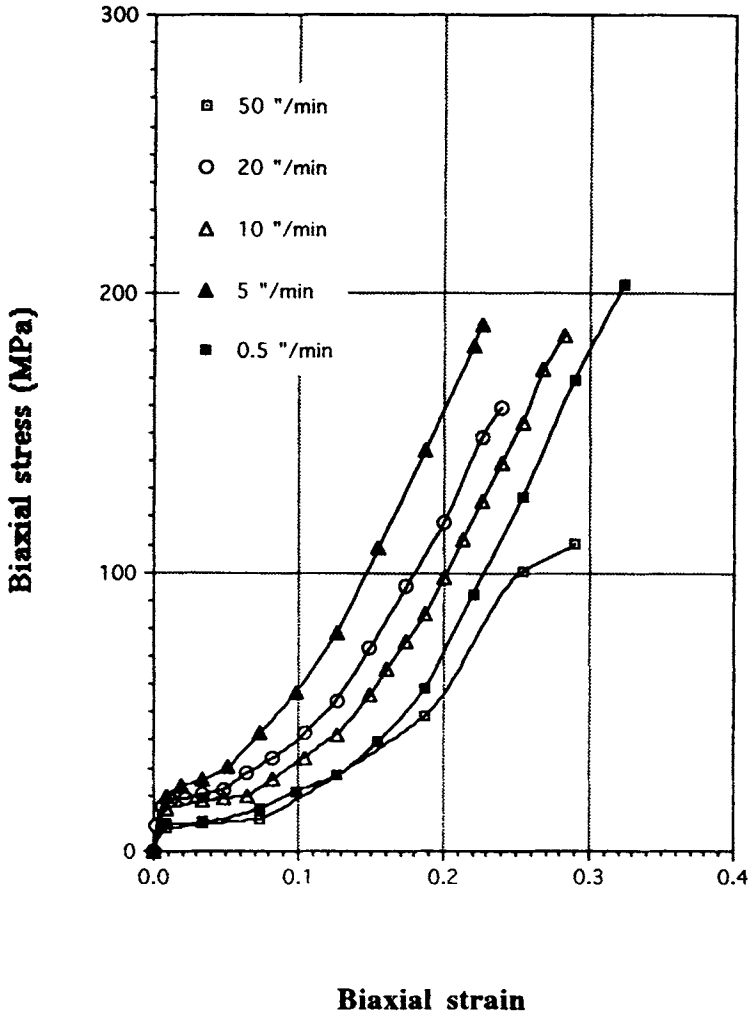

Figure 13 Biaxial stress-strain behavior in ball-burst experiments (data shown until the point of rupture).

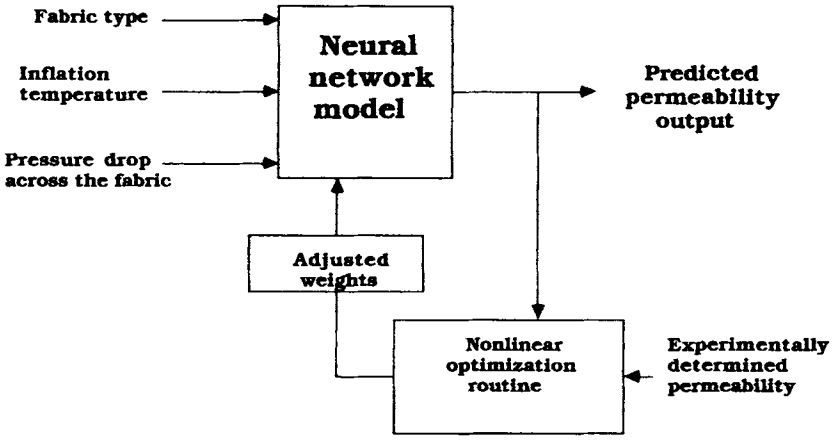

Figure 14 Schematic of the proposed neural network training for permeability predictions.

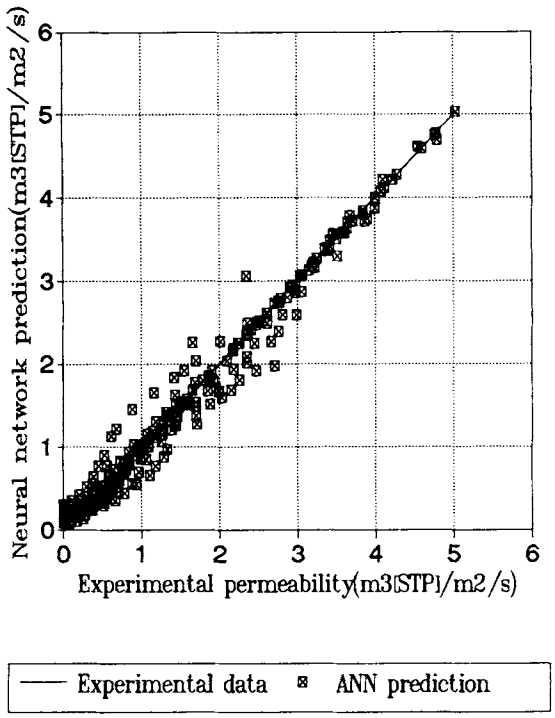

Figure 15 Neural network training of the permeability data at 281, 323, and 373 K.

ing squares of the output errors from the network is minimized. The delta rule requires that the sigmoidal function used at each neuron be continuously differentiable. This method identifies an error associated with each neuron for each iteration involving a cause–effect pattern. Therefore, the error for each neuron in the output layer can be represented as

$$\delta_{i,p} = (T_{i,p} - S_{i,p}) f'(U_{i,p}) \tag{8}$$

where $T_{i,p}$ is the desired target output for neuron i and pattern p, and f' is the derivative of the sigmoidal function used for neuron i. The change in the weight of the connection between neuron i and neuron j is given by

$$\underset{(n+1)}{\Delta} w_{i,j} = \beta(\delta_{i,p} S_{i,p}) + \alpha \underset{n}{\Delta} w_{i,j} \tag{9}$$

where β is the learning rate, α is the momentum factor, and n indexes the iteration.

The error signal from the neurons in the output layer can be easily identified. This is not so for neurons in the hidden layers. Back-propagation overcomes this difficulty by propagating the error signal backward through the network. Hence, for the hidden layers, the error signal is obtained by

$$\delta_{i,p} = f'(u_{i,p}) \sum_{j} (\delta_{j,p} w_{i,j}) \tag{10}$$

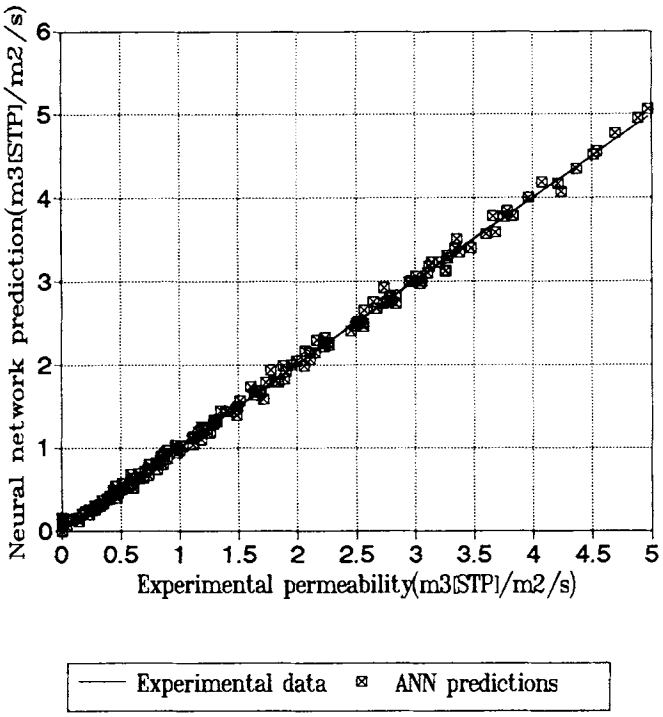

Figure 16 Neural network testing of the permeability data at 298 and 348 K.

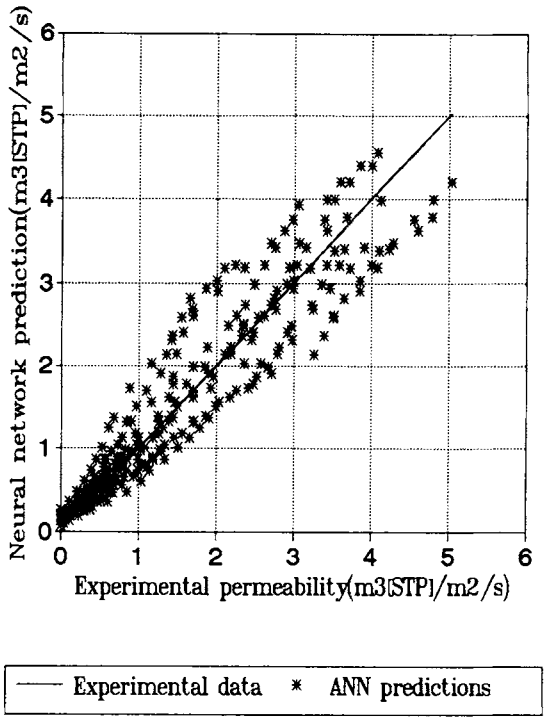

Figure 17 Neural network training results for a back-propagation training routine with conjugate-gradient search.

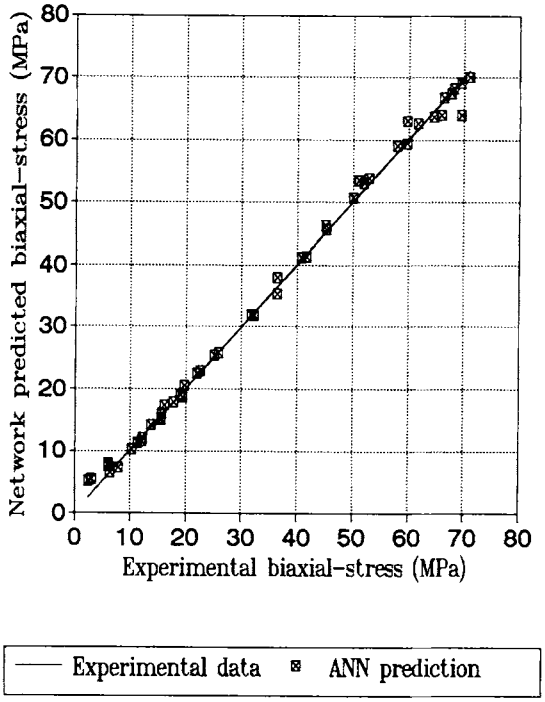

Figure 18 Neural network training of the biaxial stress-strain data.

where j represents the neurons to which neuron i in the hidden layer sends the output. Hence, the weights were updated as shown in eq. (9).

Finally, any training is incomplete without proper validation of the trained model. Therefore, the trained network should be tested with data that it has not seen. This procedure was followed in this study by first training the network on one data set and then testing it on a second different data set.

EXPERIMENTAL

Fabric Materials

In this article, the performances of four different nylon 66 fabrics were studied. The effect of the denier of the fiber, weave count, inflating gas temperature, and pressure drop across the fabric, both in terms of permeability and biaxial stress–strain, were considered in the proposed neural network model. Traditionally, nylon 66 has been the material of choice for fabrics used in safety airbag construction. In addition to the good engineering properties of their constituent fibers, fabrics must be compatible with the design constraints required in the construction and performance of airbags.

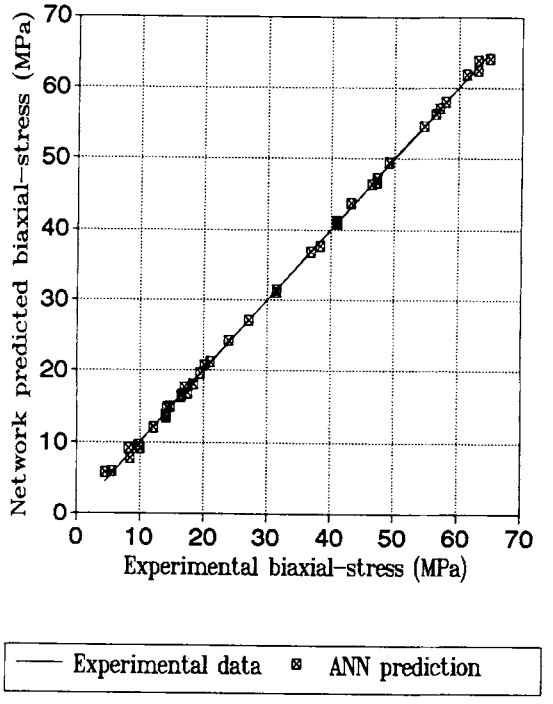

Figure 19 Neural network testing of the biaxial stress-strain data.

The nylon 66 fabrics consisted of four different deniers, i.e., 315D, 420D, 630D, and, 840D. The 315D and 630D fabrics were a plain weave, while the 420D fabric and the 840D fabric had a fancy weave and a ripstop, respectively. Their respective weave counts are given in Table I.

Blister-inflation technique

The blister-inflation technique is a quasi-steady-state measurement in which a blister is created by a pressure drop across the fabric. The fabric is maintained in this distended shape while data on permeability and biaxial strain are recorded.[1,13] These biaxial characteristics are important since they directly impact on the energy dissipation characteristics of the fabric used in smart-airbags. Moreover, the blister-inflation technique for measuring fabric permeability provides a convenient analog for stretching behavior which is very similar to that which the actual bag must undergo during deployment. When an expansible fabric is stretched biaxially by inflation into a spherical segment or "blister," the fabric's structure opens up and it becomes more permeable, just as the fabric in an airbag does when it is inflated. In this study, the performances of four different nylon 66 fabrics were examined by blister inflation.

Apparatus

In this experiment, a flat sheet of test fabric was deformed into a blister with compressed air.[1,13] A schematic diagram of the experimental apparatus is shown in Figure 3. The basic component of the apparatus is the sample-jig assembly. The sample jig itself consisted of two metal plates, both with a centered, beveled hole of diameter, D = 0.075 m. The test fabric of thickness, d_0, was clamped between the plates which were then bolted together to form a tight seal at the edge of the hole. As shown, the compressed air which was used to form the blister passed through a pressure regulator, a manual valve, a *Speedaire*® moisture trap, and a heat exchanger prior to entering the blister-jig assembly. A pressure gauge, to determine, P, was positioned in the line downstream of the moisture trap to measure the differential pressure across the inflated fabric. The blister height, h, was measured manually. The volumetric flow rate of air passing through a given test fabric for a given differential pressure drop was measured with a Taylor® anemometer. The volumetric flow was corrected to STP.

RESULTS AND DISCUSSION

Permeability Relationship

When the experimental data were plotted as permeability isotherms, the permeability of the four fabrics as a function of pressure drop remained linear over the entire pressure drop range of 0–200 kPa. However, a better insight into a fabric's characteristics is obtained from studies of the variation of permeabilities with inflating gas temperature when the data are displayed as permeability isobars. The pressure-drop range used in this study varied from 3.4 to 200 kPa. The fabrics were tested at five different isothermal temperatures: 281, 298, 323, 348, and 373 K. The experimental volumetric permeability data were corrected to STP for different pressure drops and temperature for all the experimental data. The temperature of the compressed air used for inflation was maintained with the use of a heat exchanger. The observed behaviors of different nylon fabrics are discussed under two separate sections; (1) low (0–62 kPa) pressure-drop and (2) high (62–200 kPa) pressure-drop experiments.

Low-pressure-drop Experiments

The 315D fabric was the only material that exhibited a positive increase in permeability when the temperature of the inflating gas was increased from 281 to 323°C. This is shown in Figure 4. The permeability of this fabric at and below 298 K could not be detected in the blister-inflation apparatus until a pressure drop of 13.7 kPa was attained. A maximum in permeability was observed around 323 K for the inflating gas. This peak became more obvious at pressure drops exceeding 34.4 kPa. However, with further increases in temperature above the glass transition temperature, the permeability decreased drastically. This behavior of low-denier nylon fabrics around T_g was reported in earlier publications.[14,15] We believe that with an increase in pressure and temperature above T_g the individual fiber bundles expand/swell and transform into an elliptical cross section from their initial circular cross sections, thus resulting in increase in the cover factor of the fabric.

The other three fabrics (420D, 630D, and 840D) exhibited decreasing permeabilities with increasing temperature of the inflating gas, as shown in Figures 5–7. In the case of the 420D fabric, this decline was more pronounced at 373 K. With an increase in temperature from 281 to 373 K, the permeability changed from 0.2 to 1.6 ($m^3\{STP\}/m^2/s$) for pressure drops of 3.4 and 62.0 kPa, respectively. This

behavior of a 420D fabric with a plain weave was described elsewhere.[6,16] The 630D fabric exhibited permeability only at the extremes of temperatures for a 3.4 kPa pressure drop. This material exhibited a trough in its permeability isobars with a minimum near 343 K. The permeability of the 840D fabric at a 3.4 kPa pressure drop was not detectable in the blister-inflation apparatus for temperatures below 323°C. Otherwise, this fabric exhibited a decrease in permeability with an increase in the temperature. This behavior of the 840D fabric has been eluded to elsewhere.[15] In general, the average permeability of the nylon fabrics increased with respect to temperature and pressure in the following order: 420D > 840D > 630D > 315D. In our experience, the 840D fabric was usually more permeable than was the 420D fabric if the latter had a plain weave.[15] The new fancy weave for the 420D fabric was highly permeable over the expected temperature and pressure drop levels for the 420D fabric was highly permeable over the expected temperature and pressure drop levels for airbags. This may be then ideally suited for smart-airbag applications in which vents are not used.

This measured decrease in permeability with increases in temperature of the inflating gas can introduce significant errors in models that do not incorporate these effects. Also, when trying to reduce the response time of the initial peak in the pressure–time history of airbag deployment, the temperature level at which the fabric is exposed governs the level of energy dissipation.

High-pressure-drop Experiments

The behavior of the 315D fabric with an increase in pressure drop from 62.0 to 200 kPa is shown in Figure 8. The permeability of this fabric at temperatures below room temperatures, i.e., at 281 K, was higher than the recorded permeability at room temperatures. This behavior creates a change in slope from positive to negative at higher pressure drops in this temperature range as reported in our earlier publications.[4,15] We believe that the low-denier fibers shrink with reduced temperatures and, hence, cause the stretched fabric to exhibit an increase in openness. The distinctive permeability peaks around the glass transition temperatures, T_g, for nylons (323–353 K) were more pronounced at the higher-pressure drops. Once again, however, the permeability was observed to drop drastically following temperature increases above the T_g range.

In the case of the 420D fabric, a much steeper decline in the slope of the permeability isobar was noticed with increases in temperature from 281 K to until around 323 K, as shown in Figure 9. A small peak in permeability was observed in the glass transition temperature range. But with further increases in temperature above T_g, the permeability decreased. The 630D fabric exhibited a steady decline in its permeability isobar with increases in temperature (Fig. 10). The slope of this decline was greatest in the T_g region. The performance of the 840D ripstop fabric was similar to its performance at the lower-pressure drops. A small permeability peak was observed within the glass transition temperature range when the pressure drop was above 131 kPa, as shown in Figure 11. The order of permeability remained the same for the higher-pressure-drop experiments.

Biaxial Stress–Strain Relationship

The biaxial stress–strain characteristics of the four fabric samples were determined by the blister-inflation technique. This is a quasi-steady-state measurement in which the blister is created by a pressure drop across the fabric. This technique is more sensitive in the lower biaxial strain region, i.e., when ε_b = 2–4%. The biaxial stress–strain behavior as determined by the blister-inflation technique is shown in Figure 12 for all four fabrics. Results are presented in this article only for the room-temperature evaluations. Temperature was not found to influence the biaxial stress–strain characteristics. All the experimental data points are shown connected by a interpolated line. Based on this study, it would appear that all the fabrics underwent some fiber realignment both as the pressure drop approached 27 kPa and again at higher-pressure drops depending on the type of the weave and fiber denier. A fit of the data representing biaxial stress–strain below a pressure drop of 34 kPa yielded a fabric flexural modulus of 2×10^9 kPa. This value is in the mid-range of the values reported in the literature for the flexural modulus for bulk nylon 66.[16]

Based on Figure 12, the permeability order for the different nylons becomes apparent. Among the four nylons, the 840D fabric exhibited the steepest slope, indicating a greater fabric stiffness for this material. Hence, an overall stiffness (modulus) correlates with permeability and also with the fabric's ability to be folded into compact bundles. Moreover, the divergence in behavior between the two permeability fabrics, i.e., 315D and 420D, at higher-pressure drops is indicative of the potential role that fiber movement with the yarn bundles can have on the fabric's openness as it is stretched biaxially. Finally, it is important to note that the blister-inflation

technique does not produce rupture stress–strain levels. Therefore, as a comparison, the 315D fabric's biaxial stress–strain performance obtained from ball-burst experiments is shown in Figure 13.

Permeability Predictions by the Proposed Neural Network Model

The main purpose of the study was to develop a model that can be used to predict the changes in permeability with inflation temperature and pressure drop. The network used in the model was a 3-input node, 6-hidden node, 1-output node (abbreviated as a 3-6-1 network) architecture. The permeability data were divided into two data sets: The training data set was at three temperature levels, namely, 281, 323, and 373 K. This covered the whole range of operating conditions for the 22 different isobaric pressure drops. The second, or test, data set consisted of the permeabilities obtained at the other two temperature levels, namely, 298 and 348 K. These also covered all 22 different isobaric pressure-drop conditions. The fabric characteristics incorporated in the model were the fabric type (fabric denier, weave type), the inflation temperature, and the internal pressure drop. A schematic of the proposed neural network training routine is shown in Figure 14. All the four types of nylons were trained and tested together with appropriate differentiation for each.

The training data set consisted of 264 permeability data points at three different inflation temperature levels (281, 323, and 373 K) and 22 different pressure-drop levels over a pressure range of 3.4–200 kPa. The test data set to validate the model consisted of 176 permeability data points at two different inflation temperature levels (298 and 348 K) and the same 22 pressure-drop levels.

The training and testing results from the feed forward neural network model are shown in Figures 15 and 16, respectively. The model predictions for permeability were within a ±10% error limit. This agreement is very good considering the nature of this experiment, and, also, this level of error constitutes a relatively small level of energy dissipation by viscose flow through the airbag.[3] The training of the same data set with a back-propagation routine did not converge. Hence, the real-world data was normalized by a "Z-scaling" method, which removes the constant offset common in many real-world data sets. The normalized data were then trained with the back-propagation routine; the best possible training achieved for this data is shown in Figure 17. The weights were adjusted by this method at the end of every epoch. Hence, the training was extremely slow. Further, the routine uses a gradient-descent search, which is strongly a function of the initial guess, and the training achieved was not satisfactory. The proposed nonlinear optimization-based algorithm is not only very fast in converging, but it is very efficient for highly nonlinear problems like the one under consideration in this article.

Biaxial Stress–Strain Predictions by Neural Network Model

The experimental data in this instance were randomly separated into two data sets. The training data set consisted of 48 data points and the corresponding test data set consisted of 40 data points. The effects of the type of the fabric, i.e., fabric denier and weave type, pressure drop, and biaxial strain were considered as the input layers. The predicted variable was the biaxial stress of the fabric. However, since the change in the biaxial stress–strain relationship with inflation temperature was not significant, this effect was ignored in the model. The same 3-6-1 feed forward neural network architecture was used. The training and test results from the network model are shown in Figures 18 and 19. The model predictions were within a ±1% error limit.

CONCLUSIONS

This article introduces a new approach which utilizes a feed forward neural network technique to model fabric permeability characteristics as a function of temperature and pressure drop when the fabric is under biaxial tension conditions. The proposed neural network model is conceptually simple, but its predictions were very good: well within reasonable error limits considering the complexities involved. The proposed model was capable of handling real-world data and does not require initial data processing. Further, the proposed model is extremely fast in both the training and test phases. Hence, this model has the potential to be used for on-line simulation of airbag deployment studies.

This work was sponsored by the Chrysler Challenge Fund Project No. 2002570 and State of Texas, ATP Project No. 003644-012. The authors are also indebted to Mr. John Sollars from the design center at Milliken & Company for furnishing the test samples used in this study.

REFERENCES

1. R. W. Tock and G. S. Nusholtz, *SPE, ANTEC'93 Tech. Pap.*, 1302–1306 (1993).
2. R. W. Tock and G. S. Nusholtz, *SPE, ANTEC'93 Tech. Pap.*, 2480–2486 (1993).
3. R. Keshavaraj, R. W. Tock, and G. S. Nusholtz, SAE International Congress & Exposition Conference (paper #950340), Detroit, Feb. 1995.
4. R. Keshavaraj, R. W. Tock, and G. S. Nusholtz, *J. Mech.*, to appear.
5. R. Keshavaraj, R. W. Tock, and G. S. Nusholtz, *ANTEC'94 SPE Tech. Pap.*, 2556–2559 (1994).
6. C. D. Denson, *Polym. Eng. Sci.*, **13,** 125 (1973).
7. C. D. Denson and R. J. Gallo, *Polym. Eng. Sci.*, **11,** 174 (1971).
8. D. D. Joye, G. W. Poehlein, and C. D. Denson, *Trans. Soc. Rheol.*, **16,** 142 (1972).
9. K. C. Hoover and R. W. Tock, *Polym. Eng. Sci.*, **16**(2), 82–86 (1976).
10. J. M. Zaruda, *Introduction to Artificial Neural Systems*, West, New York, 1992.
11. D. W. Marquardt, *J. Soc. Indust. Appl. Math.*, **11**(2), 431–441 (1969).
12. R. Fletcher, AERE-R 6799; Theoretical Physics Division, Atomic Energy Research Establishment: Harwell, Berkshire, U.K., 1971.
13. R. Keshavaraj, R. W. Tock, and G. S. Nusholtz, SAE International Congress & Exposition Conference (paper #950341), Detroit, Feb. 1995.
14. R. Keshavaraj, R. W. Tock, and D. Haycook, *J. Model. Simul. Mater. Sci.*, to appear.
15. R. Keshavaraj, R. W. Tock, and D. Haycook, *J. Tex. Inst.*, to appear.
16. F. Rodriquez, *Principles of Polymer Systems*, 3rd ed., Hemisphere, New York, 1989, Appendix.

Received November 3, 1994
Accepted February 25, 1995